Elliptic flow coalescence to identify the $f_0(980)$ content

An Gu,[1,*] Terrence Edmonds,[1,†] Jie Zhao,[1,‡] and Fuqiang Wang[1,2,§]

[1]*Department of Physics and Astronomy, Purdue University, West Lafayette, Indiana 47907, USA*

[2]*School of Science, Huzhou University, Huzhou, Zhejiang 313000, China*

(Received 1 March 2019; accepted 2 January 2020; published 12 February 2020)

We use a simple coalescence model to generate $f_0(980)$ particles for three configurations: a $s\bar{s}$ meson, a $u\bar{u}s\bar{s}$ tetraquark, and a K^+K^- molecule. The phase-space information of the coalescing constituents is taken from a multiphase transport (AMPT) simulation of heavy-ion collisions. It is shown that the number of constituent quarks scaling of the elliptic flow anisotropy can be used to discern $s\bar{s}$ from $u\bar{u}s\bar{s}$ and K^+K^- configurations.

DOI: 10.1103/PhysRevC.101.024908

I. INTRODUCTION

Exotic hadrons [hadrons with configurations other than the usual $q\bar{q}$ and $qqq(\bar{q}\bar{q}\bar{q})$ configurations] have been searched for a long time, since exotic hadron states are allowed by quantum chromodynamics (QCD) and therefore their studies can further our understanding of QCD [1]. The $f_0(980)$ is one of the candidate exotic hadrons, which was first observed in $\pi\pi$ scattering experiments in the 1970's [2–4]. Its configuration is still controversial—it can be a normal $s\bar{s}$ meson, a tetraquark $s\bar{s}q\bar{q}$ state, or a $K\bar{K}$ molecule [5–7].

Heavy-ion collisions create a deconfined state of quarks and gluons, called the quark-gluon plasma (QGP) [8–12]. They can provide a suitable environment to study exotic hadrons, because a large number of quarks and gluons permeate the QGP. When the temperature decreases, those quarks and gluons group into hadrons, presumably including exotic ones. This process is called hadronization and is not well understood. A common mechanism to describe hadronization in heavy-ion collisions is the quark coalescence in which several quarks (antiquarks) combine together to form a hadron [13,14]. Coalescence model was originally developed to describe the formation of deuterons from targets exposed to proton beams [15] and is extensively used to describe hadron production in relativistic heavy-ion collisions [13,16–22].

In noncentral heavy-ion collisions, the azimuthal distribution of particles is anisotropic, believed to result from hydrodynamic expansion of the initial anisotropic overlap regions [23]. The particle azimuthal distribution is often expressed in Fourier series [24]:

$$\frac{dN}{d\phi} \propto 1 + 2\sum_{n=1}^{\infty} v_n \cos[n(\phi - \psi_n)], \tag{1}$$

where ϕ is the particle azimuthal angle, ψ_n is the nth harmonic plane. The coefficients (v_n) are often called anisotropic flows, and are transverse momentum (p_T) and rapidity (y) dependent. In heavy-ion collisions, the leading anisotropic term is the $n = 2$ term because of the approximate elliptical shape of the collision overlap geometry; ψ_2 is a proxy for the unmeasured reaction plane and v_2 is called elliptic flow. If partons (quarks, antiquarks), which combine into a hadron have the same momentum, then we have

$$p_{T,h} = n_q \cdot p_{T,q}, \tag{2}$$

where n_q is the number of constituent quarks in the hadron. Keeping only v_2 in Eq. (1), we have

$$\frac{dN_h}{d\phi} \propto \left(\frac{dN_q}{d\phi}\right)^{n_q} \propto [1 + 2v_{2,q}(p_{T,q})\cos(2[\phi - \psi_{RP}])]^{n_q}$$
$$\approx 1 + n_q \cdot 2v_{2,q}(p_{T,q})\cos(2[\phi - \psi_{RP}]). \tag{3}$$

Thus, we have

$$v_{2,h}(p_{T,h}) = n_q \cdot v_{2,q}(p_{T,h}/n_q). \tag{4}$$

This result is known as the number of constituent quarks (NCQ) scaling of elliptic flow, when the momenta of the coalescing (anti)quarks are not identical, the NCQ scaling is not as good [25]. Resonance decays can cause violations, however, those violations are not severe enough to affect the qualitative feature of the NCQ scaling [26,27]. Experimentally, approximate NCQ scaling has been observed [28–34]. The elliptic flow of a hadron species can therefore tell us the number of constituent quarks contained in the hadron.

In this work, we use a coalescence model to study the elliptic flow (v_2) of the $f_0(980)$ for its different configuration assumptions. Although the string melting version of the AMPT model (a multiphase transport) [35] uses quark coalescence to form hadrons [36,37], it does not produce tetraquark hadrons. In order to simulate the production of the $f_0(980)$ for different configurations, we build our own simple coalescence model. We take the phase-space information of quarks (and Kaons) from AMPT in midcentral Au + Au collisions at 200A GeV as input to our coalescence. We use this

*gu180@purdue.edu

†tedmonds@purdue.edu

‡zhao656@purdue.edu

§fqwang@purdue.edu

simple coalescence model to generate pions, protons, kaons, ϕ mesons and $f_0(980)$ particles of three configurations ($s\bar{s}$, $u\bar{u}s\bar{s}$, $K\bar{K}$), and calculate their elliptic flow. We first compare the v_2 of pions and protons from our coalescence model with those from AMPT to validate our simple coalescence model approach. We then study the NCQ scaling of the $f_0(980)$ v_2 and demonstrate that it is a viable way to identify its quark content.

II. COALESCENCE MODEL

The main idea of the coalescence model is to combine several partons into one hadron. The model was implemented in heavy-ion collisions to describe the NCQ scaling of elliptic flow, the baryon-to-meson ratio, and the hadron transverse momentum spectra, which can not be described well by the fragmentation model [18].

Suppose N constituent particles are coalesced into a composite particle (a hadron or a $K\bar{K}$ molecule). The total yield of the composite particle can be expressed as [13]

$$N_c = g_c \int \left(\prod_{i=1}^{N} dN_i \right) f_c^W(\vec{r}_1, \dots, \vec{r}_N, \vec{p}_1, \dots, \vec{p}_N). \tag{5}$$

Here $f_c^W(\vec{r}_1, \dots, \vec{r}_N, \vec{p}_1, \dots, \vec{p}_N)$ is the Wigner function (WF), which is proportional to the coalescence probability and g_c is a statistical factor. The statistical factor g_c only affects the yield of the hadrons instead of the elliptic flow, so we set $g_c = 1$ for all kinds of hadrons in this study.

For a meson, we expect that two partons with closer distance from each other in spatial space and momentum space will have larger chance to form a meson. Thus we take the WF as Gaussian:

$$f_{\text{meson}}(\vec{r}_1, \vec{r}_2, \vec{p}_1, \vec{p}_2) = A \cdot \exp\left(-\frac{r_{12}^2}{{\sigma_r}^2} - \frac{p_{12}^2}{{\sigma_p}^2} \right), \tag{6}$$

where

$$r_{ij}^2 = (\vec{r}_i - \vec{r}_j)^2, \quad p_{ij}^2 = (\vec{p}_i - \vec{p}_j)^2. \tag{7}$$

Here, $\vec{r}_i$ and $\vec{p}_i$ are the position and momentum of ith quark/antiquark at the time the hadron is formed. If we treat partons as Gaussian wave packets, the equivalent Wigner function would appear slightly different. The reader is inferred to Ref. [38] for details. Since partons in AMPT have determined position and momentum information simultaneously, we do not use the wave packet description. In AMPT, partons freeze out (FO) [which means this (anti)quark does not interact with others anymore] at different times t_i. The moment for two or more (anti)quarks to coalesce is set to be the latest freeze-out time of those (anti)quarks, t_F. The final positions are calculated as $\vec{r}_i = \vec{r}_{i,FO} + \vec{v}_{i,FO} \times (t_F - t_{i,FO})$. For K and $\bar{K}$ particles, we take their FO phase-space information right after they are formed in AMPT.

There are two parameters in Eq. (6), A and σ_r ($\sigma_p = 1/\sigma_r$). The parameter A can be calculated from the normalization of Wigner function ($A = 8$ for two-body system [39]), since it only affects the total yield of hadrons, not the v_2, so we set it to 1. Assuming the system is in s-wave state, we have $\sigma_r = 1/\sqrt{\mu\omega}$, where μ is the reduced mass of the two-body simple harmonic oscillator system, and ω is the oscillator frequency. The oscillator frequency can be fixed by $\omega = 3/(2\mu\langle r^2\rangle)$, where $\langle r^2\rangle$ is the mean square radius of the hadron [40]. Thus, we have $\sigma_r = \sqrt{2\langle r^2\rangle/3}$. For pions, $\langle r^2\rangle = (0.61 \pm 0.15)$ fm^2 [41], so we set $\sigma_r = 0.64$ fm. For kaons, $\langle r^2\rangle = (0.34 \pm 0.05)$ fm^2 [42], we set $\sigma_r = 0.48$ fm. For ϕ mesons ($s\bar{s}$), its internal structure and radius is still not well known, and its cross section with nonstrange hadron is small [43], so we set $\sigma_r = 0.5$ fm.

For multiparticle systems, the quantum state is difficult to compute analytically. For tetraquark and pentaquark hadrons, only the heavy quark sector has been calculated quantum mechanically using perturbative approaches [44–47]. A widely used way to calculate the Wigner function can be found in Ref. [38], which is based on the assumption in the case of a baryon as an example, that the two partons form a simple harmonic oscillator (SHO) first, and then form another SHO with the third parton. In this work, for baryons and tetraquark systems, we naively define the Wigner function also to be Gaussian. For baryons,

$$\begin{aligned} &f_{\text{baryon}}(\vec{r}_1, \vec{r}_2, \vec{r}_3, \vec{p}_1, \vec{p}_2, \vec{p}_3) \\ &\quad = A \cdot \exp\left(-\frac{1}{3\sigma_r^2} \cdot \sum_{i,j=1\ i<j}^{3} r_{ij}^2 - \frac{1}{3\sigma_p^2} \cdot \sum_{i,j=1\ i<j}^{3} p_{ij}^2 \right), \end{aligned} \tag{8}$$

and for tetraquarks,

$$\begin{aligned} &f_{\text{tetra}}(\vec{r}_1, \vec{r}_2, \vec{r}_3, \vec{r}_4, \vec{p}_1, \vec{p}_2, \vec{p}_3, \vec{p}_4) \\ &\quad = A \cdot \exp\left(-\frac{1}{6\sigma_r^2} \cdot \sum_{i,j=1\ i<j}^{4} r_{ij}^2 - \frac{1}{6\sigma_p^2} \cdot \sum_{i,j=1\ i<j}^{4} p_{ij}^2 \right). \end{aligned} \tag{9}$$

For protons, $\sqrt{\langle r^2\rangle} = 0.88$ fm [48], so we set $\sigma_r = \sqrt{2\langle r^2\rangle/3} = 0.72$ fm. For the $f_0(980)$ particles, we have $\omega = 67.8$ MeV [49]. If we consider $s\bar{s}$ configuration, the reduced mass is $\mu = m_s/2$ with $m_s = 0.199$ GeV$/c^2$ [35], so $\sigma_r = 1/\sqrt{\mu\omega} = 2.4$ fm. We set this value of σ_r for all three different configurations of the $f_0(980)$. In our coalescence model, we get the freeze-out information of (anti)quarks after the parton cascade in AMPT. We input this information to our simple coalescence model to produce hadrons. We loop over all available (anti)quarks to form pions, protons, or $f_0(980)$, and we carry out the coalescence separately for each of these species. For each species, if the flavors of the (anti)quarks are correct for the hadron and the value of a random number (uniformly distributed between 0 and 1) is smaller than the value of the Wigner function, the hadron is formed. The four-momentum of the hadron is calculated as the sum of the four-momentum of its constituents, $p_h^\mu = \sum_i p_{q,i}^\mu$. And these (anti)quarks are then removed from further consideration of coalescence.

Usually in coalescence, the physical mass of hadron is directly assigned. The energy is not conserved in this process. It is pointed out in Ref. [15] that a third body may cure this deficiency. It was also pointed out that the uncertainty principle may be considered to solve this problem [50]. In our study, we produce hadrons through simple coalescence and the hadrons do not rescatter further, so the mass does not matter to our final results. Thus we do not assign the physical masses of hadrons. However, the invariant mass contains kinematic information, which may affect v_2, so we keep the information of invariant mass from the four-momentum to check the effect on our v_2 results as discussed below.

III. RESULTS

We use this simple coalescence model to generate pions, protons, kaons, ϕ mesons, and $f_0(980)$ of three different configurations ($s\bar{s}$, $u\bar{u}s\bar{s}$, K^+K^-). In each event, the elliptic flow v_2 [51,52] is calculated as:

$$v_2 = \left\langle \cos 2\left(\phi - \psi_2^{(r)}\right)\right\rangle. \tag{10}$$

Here $\psi_2^{(r)}$ is the second harmonic plane (second-order event plane) of each event in the spatial configuration space of the initial overlap geometry, and is obtained by

$$\psi_2^{(r)} = [\mathrm{atan2}(\langle r_\perp^2 \sin 2\phi_r\rangle, \langle r_\perp^2 \cos 2\phi_r\rangle) + \pi]/2, \tag{11}$$

where $r_\perp$ and ϕ_r are the polar coordinate of each initial parton before the parton cascade [53]. The resolution of $\psi_2^{(r)}$ is close to 1 due to the large initial parton multiplicity [52]. The elliptic flow shown in this study are for particles within pseudorapidity window $|\eta| < 1$.

We first compare the results of pions and protons from our coalescence model with those from AMPT. We then present the $f_0(980)$ results from our coalescence model.

A. Proton and pion

The quark masses used in our study are from the AMPT model (the same as PYTHIA program) [35]. It would be more reasonable to use the constituent quark masses [54] to take into account the effects of gluons, but as we show below, the quark masses do not significantly alter our results, so we stick to the masses used in the AMPT model.

Figure 1 shows the mass spectra of protons from our Gaussian-WF coalescence with AMPT quark masses (red line) and constituent quark masses (blue line) ($m_u = m_d =$ 0.31 GeV [54]). We can see that the invariant mass from the four-momentum does not equal to the physcial mass of hadrons.

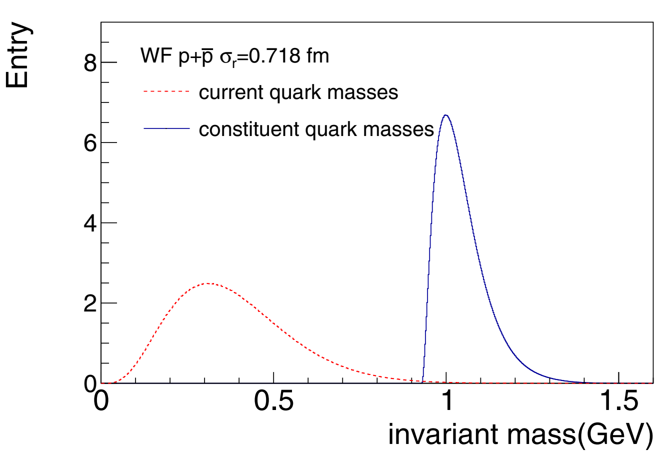

FIG. 1. Invariant mass spectra of protons from our Gaussian-WF coalescence with current quark masses (as in AMPT) and constituent quark masses, respectively. The area under each curve is normalized to 1.

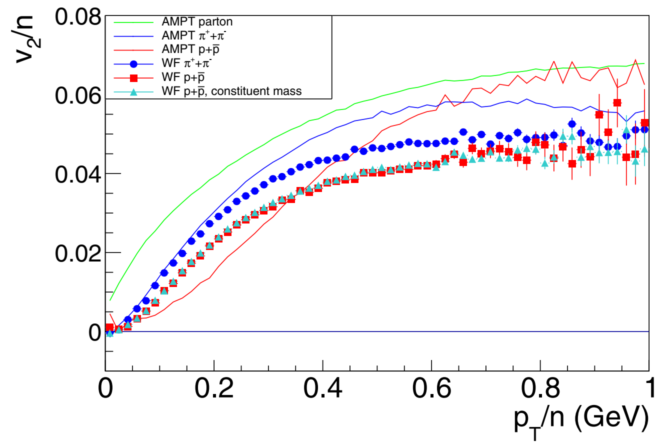

FIG. 2. v_2/n_q vs. p_T/n_q of pions and protons from Gaussian-WF coalescence compared to those from AMPT.

Figure 2 shows v_2/n_q vs. p_T/n_q for the pions (blue circle, $n_q = 2$) and protons (red square, $n_q = 3$) from our Gaussian-WF coalescence compared to those from AMPT model (blue line and red line). The pions from the Gaussian-WF coalescence have similar v_2/n_q to pions from AMPT at low p_T and lower v_2/n_q than AMPT pions at high p_T/n_q. While the WF protons have higher v_2/n_q than AMPT protons at low p_T but lower v_2/n_q at high p_T/n_q.

We checked whether the masses of quarks would affect the v_2/n_q vs. p_T/n_q by using constituent quark masses in coalescence. To do that, we simply take the AMPT quark freeze-out momenta and recalculate their velocity using constituent quark masses in propagation of quarks from freeze out to coalescence point. The result is shown in Fig. 2 where v_2/n_q vs. p_T/n_q of protons generated from our coalescence with constituent quark masses (light blue triangle) is also presented. The masses of quarks have practically no effect on the v_2/n_q. This is expected because in our simple coalescence model, the masses of quarks only affect the speeds of quarks (most relativistic), which are only related to the final spatial position of the quarks. While the v_2 only depends on the momentum of quarks, so the v_2 would be almost independent of the quark masses.

As discussed in Sec. I, the hadron mass is usually assigned in the coalescence models, not from the invariant mass of the coalescing quarks. However, the invariant mass contains the quark kinematics, and may affect their v_2. To check this, we apply invariant mass cut on protons and pions from our Gaussian-WF coalescence as shown in Fig. 3. Generally, hadrons with larger invariant masses have less v_2 since their constituent quarks are farther away from each other in momentum space. When mass <0.2 GeV is applied to pions and mass >0.4 GeV is applied to protons from the Gaussian-WF coalescence, our simple coalescence model gives more consistent results with those from the coalescence model used in the AMPT. This is not a surprise because the invariant mass is utilized by AMPT coalescence to assign hadron types [35].

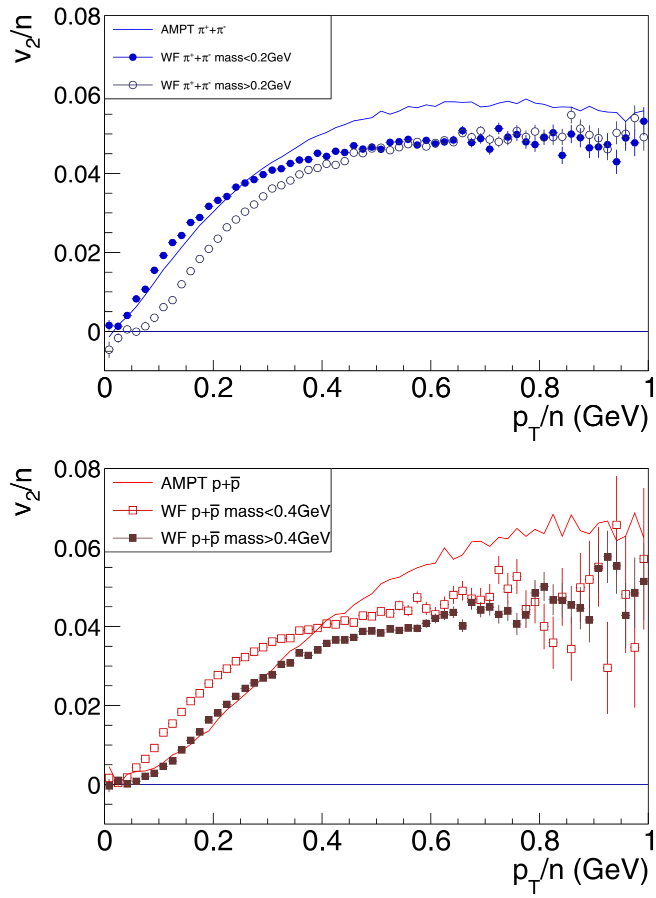

FIG. 3. v_2/n_q vs. p_T/n_q of pions (top) and protons (bottom) from Gaussian-WF coalescence for different mass cuts, compared to AMPT results.

It is also an indication that our simple coalescence model is doing a reasonable job.

As mentioned in Sec. I, the NCQ scaling is best satisfied when the coalescing partons have the same momentum. When their momenta differ, the NCQ will not be as good. Since the smaller the σ_r the larger their momentum difference ($\sigma_p = 1/\sigma_r$), we expect the goodness of the NCQ scaling to increase with σ_r. Thus we artificially change the σ_r of the proton and check how the proton v_2/n_q vs. p_T/n_q changes relative to the light quark v_2. This is shown in Fig. 4. Indeed, we observe that protons with larger value of σ_r have closer v_2/n_q vs. p_T/n_q to that of the $u(\bar{u})$, $d(\bar{d})$ quarks, i.e., closer to the ideal situation of NCQ scaling of elliptic flow ($\sigma_p \to 0$). Likewise it is reasonable for the pions and protons to have different v_2/n_q vs. p_T/n_q from the quarks as shown in Fig. 2 because of the relatively small values of σ_r. Such property of coalescence model is qualitatively consistent with the results in Ref. [39].

It is interesting to notice that although protons are generated with larger σ_r ($\sigma_r = 0.72$ fm) than the pions ($\sigma_r = 0.64$ fm), the $v_2/n_q(p_T/n_q)$ of protons is lower than that of pions. This is because there are more constituent quarks in a proton than a pion. So there is a larger reduction in v_2 from the ideal NCQ scaling picture. That is to say, in our Gauss-WF

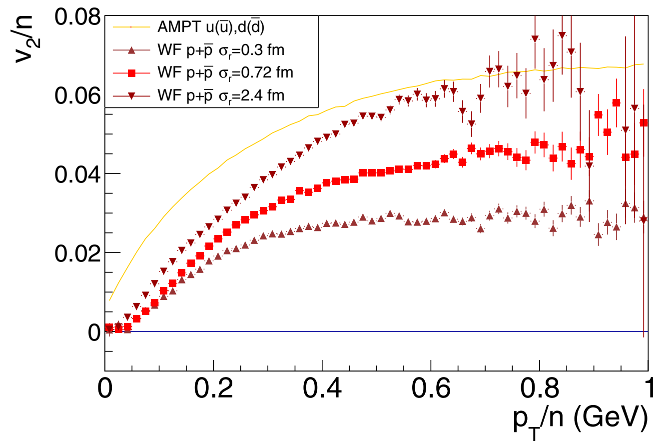

FIG. 4. v_2/n_q vs. p_T/n_q of protons generated with different values of σ_r from our WF-Gaussian coalescence, compared to that of light quarks from AMPT.

coalescence model, hadrons containing more constituents will have lower $v_2/n_q(p_T/n_q)$ for a given limited value of σ_r.

B. $f_0(980)$ particle for three configurations ($s\bar{s}$, $u\bar{u}s\bar{s}$, K^+K^-)

Figure 5 shows v_2/n_q vs. p_T/n_q ($n_q = 4$) for the tetraquark state of $f_0(980)$ from our Gaussian-WF coalescence for different mass cuts. The invariant mass distribution of $f_0(980)$ in tetraquark state from our Gaussian-WF coalescence is shown in the insert. The mass spectrum of $f_0(980)$ does not peak at 980 MeV. Using larger constituent quark masses could improve the situation. But again, the hadron mass is a known problem in coalescence, and would require better understanding of the hadronization process, which is out of the scope of this work. Similar to the protons shown in Fig. 3, the mass cut does not significantly change the $v_2/n_q(p_T/n_q)$ of $f_0(980)$ either.

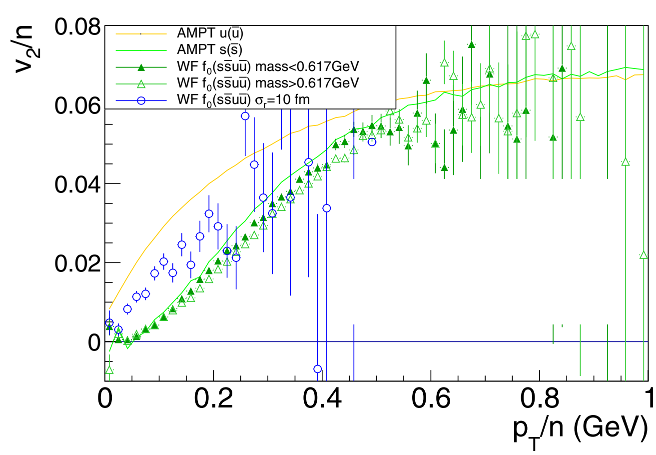

FIG. 5. v_2/n_q vs. p_T/n_q, for the tetraquark state of $f_0(980)$ from our Gaussian-WF coalescence ($\sigma_r = 2.4$) fm for different mass cuts. For comparison, the $f_0(980)$ results with $\sigma_r = 10$ fm are also shown. The curves show the results of light and strange quarks from AMPT.

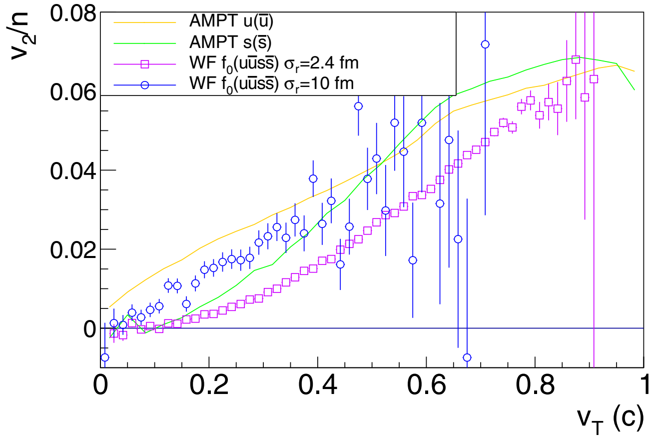

FIG. 6. v_2/n_q vs. v_T, for the tetraquark state of $f_0(980)$ from our Gaussian-WF coalescence for constituent quark masses and different values of σ_r. The curves are the results of up quark and strange quark from AMPT calculated by using constituent quark masses.

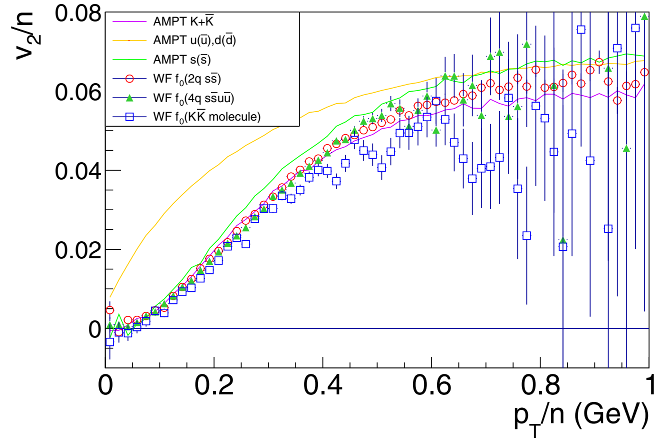

FIG. 7. v_2/n_q vs. p_T/n_q for different configurations of $f_0(980)$ from our Gaussian-WF coalescence compared to the kaon result from AMPT.

For comparison, the v_2 vs. p_T of light quark and strange quark from AMPT are also shown in Fig. 5. It is interesting to note that the $v_2/n_q(p_T/n_q)$ of the $f_0(980)(u\bar{u}s\bar{s})$ is lower than those of u quarks and s quarks, whereas one would naively expect that the $f_0(980)(u\bar{u}s\bar{s})$ results to be midway between u-quarks and s-quarks curves. In the ideal NCQ scaling picture, all the coalesced quarks in the hadron possess the same momentum, i.e. $\sigma_p \to 0$ and $\sigma_r \to \infty$. Hence the v_2/n_q of $f_0(u\bar{u}s\bar{s})$ should be $(v_{2,u\bar{u}} + v_{2,s\bar{s}})/2$ because:

$$\begin{aligned}\frac{dN_{f_0(980)(u\bar{u}s\bar{s})}}{d\phi} &\propto [1 + 2v_{2,u}(p_{T,u})\cos(2[\phi - \psi_{RP}])]^2 \\ &\quad \times [1 + 2v_{2,s}(p_{T,s})\cos(2[\phi - \psi_{RP}])]^2 \\ &\approx 1 + 2\cdot[2v_{2,u}(p_{T,f_0(980)}/4) \\ &\quad + 2v_{2,s}(p_{T,f_0(980)}/4)] \times \cos(2[\phi - \psi_{RP}]).\end{aligned} \tag{12}$$

To test this, we artificially set σ_r to a large value ($\sigma_r =$ 10 fm) to mimic the ideal NCQ scaling picture. The results are shown in Fig. 5 as the blue open circles. Indeed, the $v_2(p_T/n_q)$ of the $f_0(u\bar{u}s\bar{s})$ lies midway between those of u quarks and s quarks as expected in the ideal picture.

In coalescence, one often considers the velocities of the constituents. In order to examine the elliptic flow as a function of velocity, we use the large constituent quark masses ($m_u =$ 0.31 GeV, $m_s = 0.5$ GeV) to produce the $f_0(980)(u\bar{u}s\bar{s})$. Similar to the protons, the $v_2/n_q(p_T/n_q)$ of $f_0(980)(u\bar{u}s\bar{s})$ using constituent quark masses is almost as same as that using current quark masses (PYTHIA quark mass). The v_2/n_q of $f_0(980)(u\bar{u}s\bar{s})$ as a function of transverse velocity v_T is show in Fig. 6 together with those of constituent u quarks and s quarks. When σ_r of $f_0(980)(u\bar{u}s\bar{s})$ is set to 10 fm, the $v_2/n_q(v_T)$ also lies midway between those of u quarks and s quarks as expected in the ideal picture. The $v_2/n_q(v_T)$ is qualitatively similar to the $v_2/n_q(p_T/n_q)$ shown in Fig. 5. This is because the constituent masses of u quarks and s quarks are not very different. It should be noted, however, that in our Gauss-WF coalescence model, it is the momentum, not the velocity that is used to calculate the coalescence probability. Hence, the momentum is the more relevant variable to use than the velocity.

The above results indicate that our coalescence model is doing a reasonable job to produce tetraquark hadrons. In the following, we use our coalescence model to produce the $f_0(980)$ of the other two configurations ($s\bar{s}$ and $K\bar{K}$) and compare the elliptic flows of these three configurations.

In Fig. 7, we compare v_2/n_q vs. p_T/n_q of different configurations of $f_0(980)$. The v_2/n_q is almost the same for different configurations ($s\bar{s}$, $u\bar{u}s\bar{s}$, K^+K^-). It is easy to understand why $f_0(980)(K^+K^-)$ ($n_q = 4$) has the same $v_2/n_q(p_T/n_q)$ as the $f_0(980)(s\bar{s})$ ($n_q = 2$). This is because they are both from the two-body coalescence with the same value of σ_r, and because in AMPT kaons ($n_q = 2$) have almost the same $v_2/n_q(p_T/n_q)$ as that of the strange quarks ($n_q = 1$).

However, it is somewhat surprising that the $v_2/n_q(p_T/n_q)$ of $f_0(u\bar{u}s\bar{s})$ is almost the same as that of $f_0(s\bar{s})$. As we have previously pointed out that in our Gauss-WF coalescence model, for a given value of σ_r, hadrons containing more constituents will have lower $v_2/n_q(p_T/n_q)$. Thus we would expect the $v_2/n_q(p_T/n_q)$ of $f_0(u\bar{u}s\bar{s})$ to be lower than that of the $f_0(s\bar{s})$, which is not true here. This is because of another effect, i.e., the u quarks that $f_0(u\bar{u}s\bar{s})$ contains have larger $v_2/n_q(p_T/n_q)$ and upraise that of the $f_0(u\bar{u}s\bar{s})$. As a result, the $f_0(980)$ of $u\bar{u}s\bar{s}$ and $s\bar{s}$ configurations happen to have almost the same $v_2/n_q(p_T/n_q)$.

The common dependence of the v_2/n_q vs. p_T/n_q in Fig. 7 indicates that the NCQ scaling of $f_0(980)$ can be used to tell its number of constituent quarks. This is more evidently shown in Fig. 8 where the v_2 is directly shown as a function of p_T. The $v_2(p_T)$ of $f_0(980)$ with ($s\bar{s}$) configuration is very different from the other configurations, especially when $p_T > 1$ GeV. So according to our simple coalescence model, experimental measurement of v_2 can tell whether f_0 particle is composed of two quarks. It is, however, difficult to tell the difference between the four-quark configuration and K^+K^- molecule configuration. This is not

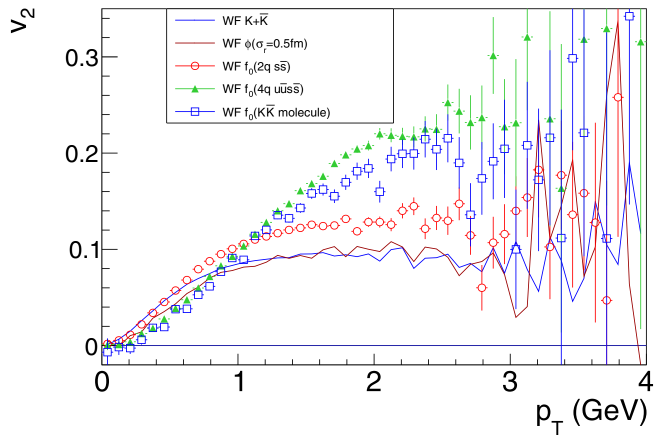

FIG. 8. v_2 vs. p_T, for kaons, ϕ, and three different configurations of $f_0(980)$ from our Gaussian-WF coalescence model.

surprising because the K^+K^- molecule is effectively a four-quark state.

Studying the yield of exotic hadrons in heavy-ion collisions using the coalescence model is another way to discriminate between different configurations. It is shown that the yield of an exotic hadron (such as a tetraquark state) is significantly smaller than the yield of a nonexotic hadron with normal number of constituent quarks [49]. This can be used to further separate tetraquark $f_0(980)$ from a K^+K^- molecule state.

Obviously, the experimental measurement of $f_0(980)$ is difficult because of the large combinatorial background of $\pi^+\pi^-$ pairs. One of the commonly used methods is to subtract like-sign pair mass spectrum from the unlike-sign one. With $\sim 10^8$ minimum bias p + p collisions, a clear $f_0(980)$ peak was observed by the ALICE Collaboration at the LHC [55]. With 1.2×10^6 Au+Au collisions in the 40–80 % centrality range, the yield of $f_0(980)$ was measured by the STAR Collaboration at RHIC [56]. With increased event samples now available, it is possible to measure the yield of $f_0(980)$ as a function of the azimuthal angle relative to the second-order event-plane to extract the v_2 of $f_0(980)$.

IV. CONCLUSION

We used a simple coalescence model with Gaussian Wigner function to generate pions, protons, kaons, ϕ mesons, and $f_0(980)$ particles of three different configurations ($s\bar{s}$, $u\bar{u}s\bar{s}$, K^+K^-). The NCQ scaling of elliptic flow v_2 is observed in our study, and can be used to distinguish the $s\bar{s}$ state of the $f_0(980)$ from the tetraquark ($u\bar{u}s\bar{s}$) or K^+K^- molecule state in heavy-ion collisions. It is difficult to tell apart the $u\bar{u}s\bar{s}$ and K^+K^- states by measuring v_2. The $f_0(980)$ yields needs to be exploited.

ACKNOWLEDGMENTS

We thank Dr. Pengfei Zhuang and Dr. Zi-wei Lin for fruitful discussions. This work was supported in part by the U.S. Department of Energy (Grant No. de-sc0012910) and the National Natural Science Foundation of China (Grant No. 11847315).

[1] R. L. Jaffe, Phys. Rep. **409**, 1 (2005).
[2] S. D. Protopopescu, M. Alston-Garnjost, A. Barbaro-Galtieri, S. M. Flatte, J. H. Friedman, T. A. Lasinski, G. R. Lynch, M. S. Rabin, and F. T. Solmitz, Phys. Rev. D **7**, 1279 (1973).
[3] B. Hyams *et al.*, Nucl. Phys. B **64**, 134 (1973).
[4] G. Grayer *et al.*, Nucl. Phys. B **75**, 189 (1974).
[5] D. V. Bugg, Phys. Rep. **397**, 257 (2004).
[6] E. Klempt and A. Zaitsev, Phys. Rep. **454**, 1 (2007).
[7] J. R. Pelaez, Phys. Rep. **658**, 1 (2016).
[8] K. Adcox *et al.* (PHENIX Collaboration), Nucl. Phys. A **757**, 184 (2005).
[9] I. Arsene *et al.* (BRAHMS Collaboration), Nucl. Phys. A **757**, 1 (2005).
[10] B. B. Back *et al.*, Nucl. Phys. A **757**, 28 (2005).
[11] J. Adams *et al.* (STAR Collabration), Nucl. Phys. A **757**, 102 (2005).
[12] B. Muller, J. Schukraft, and B. Wyslouch, Ann. Rev. Nucl. Part. Sci. **62**, 361 (2012).
[13] C. B. Dover, U. W. Heinz, E. Schnedermann, and J. Zimanyi, Phys. Rev. C **44**, 1636 (1991).
[14] R. J. Fries, V. Greco, and P. Sorensen, Ann. Rev. Nucl. Part. Sci. **58**, 177 (2008).
[15] S. T. Butler and C. A. Pearson, Phys. Rev. **129**, 836 (1963).
[16] R. C. Hwa and C. B. Yang, Phys. Rev. C **67**, 034902 (2003).
[17] R. J. Fries, B. Muller, C. Nonaka, and S. A. Bass, Phys. Rev. Lett. **90**, 202303 (2003).
[18] R. J. Fries, B. Muller, C. Nonaka, and S. A. Bass, Phys. Rev. C **68**, 044902 (2003).
[19] V. Greco, C. M. Ko, and P. Levai, Phys. Rev. Lett. **90**, 202302 (2003).
[20] V. Greco, C. M. Ko, and P. Levai, Phys. Rev. C **68**, 034904 (2003).
[21] R. C. Hwa and C. B. Yang, Phys. Rev. C **70**, 024905 (2004).
[22] V. Minissale, F. Scardina, and V. Greco, Phys. Rev. C **92**, 054904 (2015).
[23] J.-Y. Ollitrault, Phys. Rev. D **46**, 229 (1992).
[24] S. Voloshin and Y. Zhang, Z. Phys. C **70**, 665 (1996).
[25] D. Molnar and S. A. Voloshin, Phys. Rev. Lett. **91**, 092301 (2003).
[26] V. Greco and C. M. Ko, Phys. Rev. C **70**, 024901 (2004).
[27] X. Dong, S. Esumi, P. Sorensen, N. Xu, and Z. Xu, Phys. Lett. B **597**, 328 (2004).
[28] J. Adams *et al.* (STAR Collaboration), Phys. Rev. Lett. **92**, 052302 (2004).
[29] J. Adams *et al.* (STAR Collaboration), Phys. Rev. C **72**, 014904 (2005).
[30] J. Adams *et al.* (STAR Collaboration), Phys. Rev. Lett. **95**, 122301 (2005).
[31] A. Adare *et al.* (PHENIX Collaboration), Phys. Rev. Lett. **98**, 162301 (2007).
[32] B. I. Abelev *et al.* (STAR Collaboration), Phys. Rev. Lett. **99**, 112301 (2007).

[33] L. Adamczyk *et al.* (STAR Collaboration), Phys. Rev. C **88**, 014902 (2013).
[34] B. B. Abelev *et al.* (ALICE Collaboration), JHEP 06 (2015) 190.
[35] Z.-W. Lin, C. M. Ko, B.-A. Li, B. Zhang, and S. Pal, Phys. Rev. C **72**, 064901 (2005).
[36] Z.-W. Lin and D. Molnár, Phys. Rev. C **68**, 044901 (2003).
[37] Y. He and Z.-W. Lin, Phys. Rev. C **96**, 014910 (2017).
[38] K. C. Han, R. J. Fries, and C. M. Ko, Phys. Rev. C **93**, 045207 (2016).
[39] L.-W. Chen and C. M. Ko, Phys. Rev. C **73**, 044903 (2006).
[40] A. J. Baltz and C. Dover, Phys. Rev. C **53**, 362 (1996).
[41] G. Adylov, F. Aliev, D. Bardin, W. Gajewski, I. Ion, B. Kulakov, G. Micelmacher, B. Niczyporuk, T. Nigmanov, E. Tsyganov, M. Turala, A. Vodopianov, K. Wala, E. Dally, D. Drickey, A. Liberman, P. Shepard, J. Tompkins, C. Buchanan, and J. Poirier, Phys. Lett. B **51**, 402 (1974).
[42] S. R. Amendolia *et al.*, Phys. Lett. B **178**, 435 (1986).
[43] A. Shor, Phys. Rev. Lett. **54**, 1122 (1985).
[44] A. Ali, J. S. Lange, and S. Stone, Prog. Part. Nucl. Phys. **97**, 123 (2017).
[45] H.-X. Chen, W. Chen, X. Liu, and S.-L. Zhu, Phys. Rep. **639**, 1 (2016).
[46] D. M. Brink and F. Stancu, Phys. Rev. D **57**, 6778 (1998).
[47] S. Shi, X. Guo, and P. Zhuang, Phys. Rev. D **88**, 014021 (2013).
[48] A. Antognini, F. D. Amaro, F. Biraben, J. M. R. Cardoso, D. S. Covita, A. Dax, S. Dhawan, L. M. P. Fernandes, A. Giesen, T. Graf, T. W. Hänsch, P. Indelicato, L. Julien, C. Y. Kao, P. Knowles, F. Kottmann, E.-O. L. Bigot, Y.-W. Liu, J. A. M. Lopes, L. Ludhova, C. M. B. Monteiro, F. Mulhauser, T. Nebel, F. Nez, P. Rabinowitz, J. M. F. dos Santos, L. A. Schaller, K. Schuhmann, C. Schwob, D. Taqqu, J. F. C. A. Veloso, and R. Pohl, J. Phys.: Conf. Ser. **312**, 032002 (2011).
[49] S. Cho, T. Furumoto, T. Hyodo, D. Jido, C. M. Ko, S. H. Lee, M. Nielsen, A. Ohnishi, T. Sekihara, S. Yasui, and K. Yazaki (ExHIC Collaboration), Phys. Rev. Lett. **106**, 212001 (2011).
[50] S. Mrowczynski, J. Phys. G **13**, 1089 (1987).
[51] A. M. Poskanzer and S. A. Voloshin, Phys. Rev. C **58**, 1671 (1998).
[52] K. Xiao, F. Liu, and F. Wang, Phys. Rev. C **87**, 011901(R) (2013).
[53] J.-Y. Ollitrault, Phys. Rev. D **48**, 1132 (1993).
[54] V. Borka Jovanovic, S. R. Ignjatovic, D. Borka, and P. Jovanovic, Phys. Rev. D **82**, 117501 (2010).
[55] A. Lorenzo (ALICE), Nucl. Phys. A **982**, 201 (2019).
[56] P. Fachini *et al.* (STAR Collaboration), J. Phys. G **30**, S565 (2003).